The ISO/SWS spectum of IRC+10216: the vibrational bands of C2H2 and HCN

Cernicharo, J.; Yamamura, I.; Gonzalez-Alfonso, E.; de Jong, T.; Heras, A.M.; Escribano, R.; Ortigoso, J.

Published in:
Astrophysical Journal

DOI:
10.1086/312360

THE ASTROPHYSICAL JOURNAL, 526:L41–L44, 1999 November 20

THE *ISO*/SWS SPECTRUM OF IRC +10216: THE VIBRATIONAL BANDS OF C_2H_2 AND HCN[1]

JOSÉ CERNICHARO,[2] ISSEI YAMAMURA,[3] EDUARDO GONZÁLEZ-ALFONSO,[2] TEIJE DE JONG,[3,4]
ANA HERAS,[5] RAFAEL ESCRIBANO,[2] AND JUAN ORTIGOSO[2]
Received 1999 July 20; accepted 1999 September 13; published 1999 October 19

ABSTRACT

We present the *Infrared Space Observatory*/Short-Wavelength Spectrometer full grating resolution spectrum of IRC +10216, which is dominated by strong absorption/emission bands of C_2H_2 and HCN. All C_2H_2 bands and the strong near-infrared stretching bands of HCN are observed in absorption, whereas the fundamental, hot, and combination bands of HCN involving the ν_2 bending mode around 14 μm are observed in emission. Particularly strong is the HCN $\nu_2 = 2^0 \rightarrow \nu_2 = 1^1$ vibrational transition at 14.3 μm. The most plausible mechanism for such emission is the radiative pumping of molecules from the ground to the $\nu_2 = 2^0$ state (7.1 μm) followed by radiative decay: $\nu_2 = 2^0 \rightarrow \nu_2 = 1^1$. We present detailed models for HCN that verify the efficiency of the mentioned effect. The HCN abundance inferred from these models is (1.5–3) $\times$ 10^{-5}.

Subject headings: circumstellar matter — infrared: stars — radiative transfer — stars: AGB and post-AGB — stars: atmospheres — stars: individual (IRC +10216)

1. INTRODUCTION

IRC +10216 is the brightest C-rich, evolved object in the sky. It has an extended circumstellar envelope (CSE) in which around 50 molecular species have been detected, and it is probably one of the best-studied stellar objects at infrared and radio wavelengths (Cernicharo, Guélin, & Kahane 1999). IRC +10216 has a particularly rich carbon chemistry, and most molecular species are carbon-chain radicals (Cernicharo & Guélin 1996) that are formed in the external layers of the CSE (Guélin, Lucas, & Cernicharo 1993). Other species of interest detected in IRC +10216 include silicon carbide (SiC; Cernicharo et al. 1989) and the metal halides NaCl, AlCl, AlF, and KCl (Cernicharo & Guélin 1987). Some metal-bearing species are also detected in the external shell of IRC +10216, e.g., MgNC (Guélin et al. 1993). While polar molecules can be detected at radio wavelengths, nonpolar molecules can only be detected in the infrared through their active ro-vibrational transitions.

We present in this Letter a full grating resolution spectrum of IRC +10216 taken with the *Infrared Space Observatory* (*ISO*)/Short-Wavelength Spectrometer (SWS; de Graauw et al. 1996). It covers the 2.38–45 μm range with a spectral resolution of $\simeq$2000. In this work, attention will be confined to the molecular species that most strongly contribute to the emission/absorption spectrum of IRC +10216 in the near- and mid-infrared: C_2H_2 and HCN (see Cernicharo 1998). A detailed scheme for the radiative pumping of the vibrational levels of HCN is proposed.

2. OBSERVATIONS AND RESULTS

The full range AOT06 spectrum of IRC +10216 was taken on 1996 June 2 (ϕ = 0.3). Another grating spectrum with lower spectral resolution (AOT01, speed 4) was taken 2 days before. The data have been reduced with the SWS Interactive Analysis system. The very strong signal of IRC +10216 causes significant fringes in band 3 (12–28 μm) and memory effects in bands 2 (4–12 μm) and 4 (29–45.2 μm). Nevertheless, the AOT06 and AOT01 spectra can be compared to ascertain the reality of the observed features. Fringes in band 3 (12–29 μm) are removed by shifting the relative spectral responsivity function slightly in wavelength. Fringes still remaining after this procedure were removed by a fast Fourier transform method. There are small discrepancies in flux between the different bands in the spectrum. Such inconsistencies have been corrected by scaling each band with respect to bands 1b (2.6–3.0 μm) and 3d (19.5–27.5 μm), which are adopted as references.

Figure 1 shows the spectrum of IRC +10216 between 2.4 and 197 μm; it shows the 11 μm band due to SiC dust and the prominent "30 μm feature" usually attributed to MgS (Yamamura et al. 1998). A crude fit to the dust emission provides an estimate for the mass-loss rate of a few times $10^{-5}\,M_\odot$ yr^{-1}. Figure 2 shows the spectrum, normalized to the continuum flux, of IRC +10216 around 3 μm. The broad absorption feature is due to the stretching modes of C_2H_2 and HCN. In addition, the *Q*-branches of the $\nu_3+\nu_5$, $\nu_3+\nu_4$, and $\nu_2+2\nu_4+\nu_5$ modes of C_2H_2 are detected around 2.5 μm. Many combination bands of the same molecule, like $\nu_2+\nu_5$ among others, are detected around 3.8 μm. The *Q*-branch of the $\nu_2+\nu_3$ mode of HCN and those of the $\nu_1+\nu_2$ and $\nu_1+2\nu_2-\nu_2$ vibrational transitions of HCN are detected in absorption around 2.5 and 3.6 μm, respectively. The $\nu_3-\nu_2$ mode of HCN and other combination bands are also seen in Figure 2. However, they seem to be in emission rather than in absorption (see below).

Figure 3 shows the 14 μm spectrum of IRC +10216. The absorption features are due to the ν_5 bending mode of acetylene and its associated hot and combination bands. This figure shows that the HCN bands appear in emission with the *Q*-branch of the $2\nu_2^0-\nu_2^1$ transition being particularly strong. Many other weak bands are also present in the 2.4–9 and 15–25 μm ranges. However, instrumental problems preclude at the present the definite assignation of these features to real spectral bands.

[1] Based on observations with *ISO*, an ESA project with instruments funded by ESA member states (especially the PI countries: France Germany, the Netherlands, and the United Kingdom) and with the participation of ISAS and NASA.

[2] Consejo Superior de Investigaciones Científicas, Instituto de Estructura de la Materia, Departmento Física Molecular, Serrano 121, E-28006 Madrid, Spain; cerni@astro.iem.csic.es.

[3] Astronomical Institute "Anton Pannekoek," University of Amsterdam, Kruislaan 403, 1098 SJ, Amsterdam, Netherlands.

[4] SRON-Utrecht, Sorbonnelaan 2, 3584 CA Utrecht, Netherlands.

[5] Astrophysics Division, Space Science Department of ESA, ESTEC, P.O. Box 299, 2200 AG Noordwijk, Netherlands.

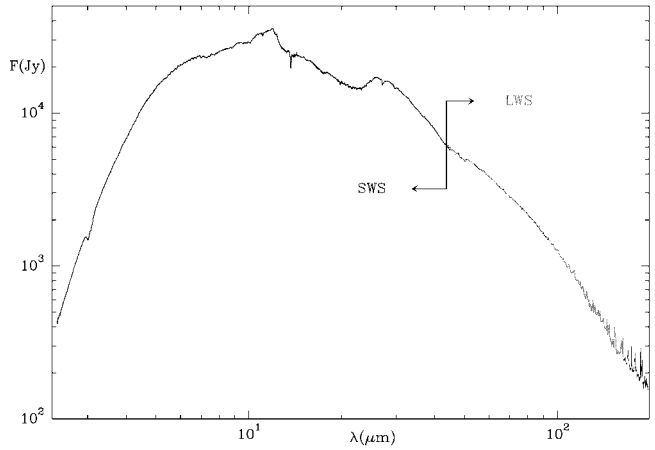

FIG. 1.—Spectrum of IRC +10216 between 2.4 and 197 μm as observed with the *ISO*/SWS and *ISO*/LWS spectrometers. At long wavelengths, the pure rotational lines of CO and HCN are clearly superposed over the weak continuum (see Cernicharo et al. 1996).

Future data products from improved calibration are needed to unambiguously derive the nature of observed features and to assign them to new species or to abundant molecules already detected in IRC +10216 such as SiS, NH_3, CH_4, and SiH_4, which have been observed in the infrared (see, e.g., Boyle et al. 1994; Keady & Ridgway 1993).

3. DISCUSSION

Observations of many C_2H_2 ro-vibrational lines at 3 and 14 μm with high spectral resolution have been reported by Ridgway, Carbon, & Hall (1978), Keady & Hinkle (1988), and Keady & Ridgway (1993). Although our data suffer from lower spectral resolution, we avail of the observations from all the C_2H_2 bands (Figs. 1 and 2), thus allowing a better estimate of the temperature of the emitting/absorbing gas and the pumping mechanisms prevailing in the innermost region of the CSE. A first attempt to fit the absorption with the ν_3 and $\nu_2+\nu_4+\nu_5$ bands of C_2H_2 (μ = 0.061 and 0.067 D; Rinsland, Baldacci, & Rao 1982) and with the ν_3 band of HCN indicated that the contribution from several hot and combination bands of C_2H_2, together with bands from $H^{13}CCH$ [$x(C_2H_2)/x(H^{13}CCH) \simeq 22$; Cernicharo et al. 1991], should be included. By assuming an LTE distribution of the C_2H_2 and HCN levels' population, we have modeled the absorption produced by the ν_3 and $\nu_2+\nu_4+\nu_5$ bands and all the hot bands arising from ν_4 = 1, 2, ν_5 = 1, 2, and $\nu_4+\nu_5$. In total we have included in our models 21 bands of C_2H_2 and two bands of $H^{13}CCH$, together with three bands of HCN and the ν_3 band of $H^{13}CN$.

A model with a single layer cannot explain the observed band profile (see Keady & Hinkle 1988). The adopted model, which is a simplification of the detailed CSE structure derived by Keady & Hinkle, includes several layers between 1 and 500 stellar radii. Figure 2 shows the best fit to the band shape at 3 μm. We have adopted $X(C_2H_2) = 5 \times 10^{-5}$ and $X(HCN) = 3 \times 10^{-5}$ (Cernicharo et al. 1996; Wiedemann et al. 1991). In

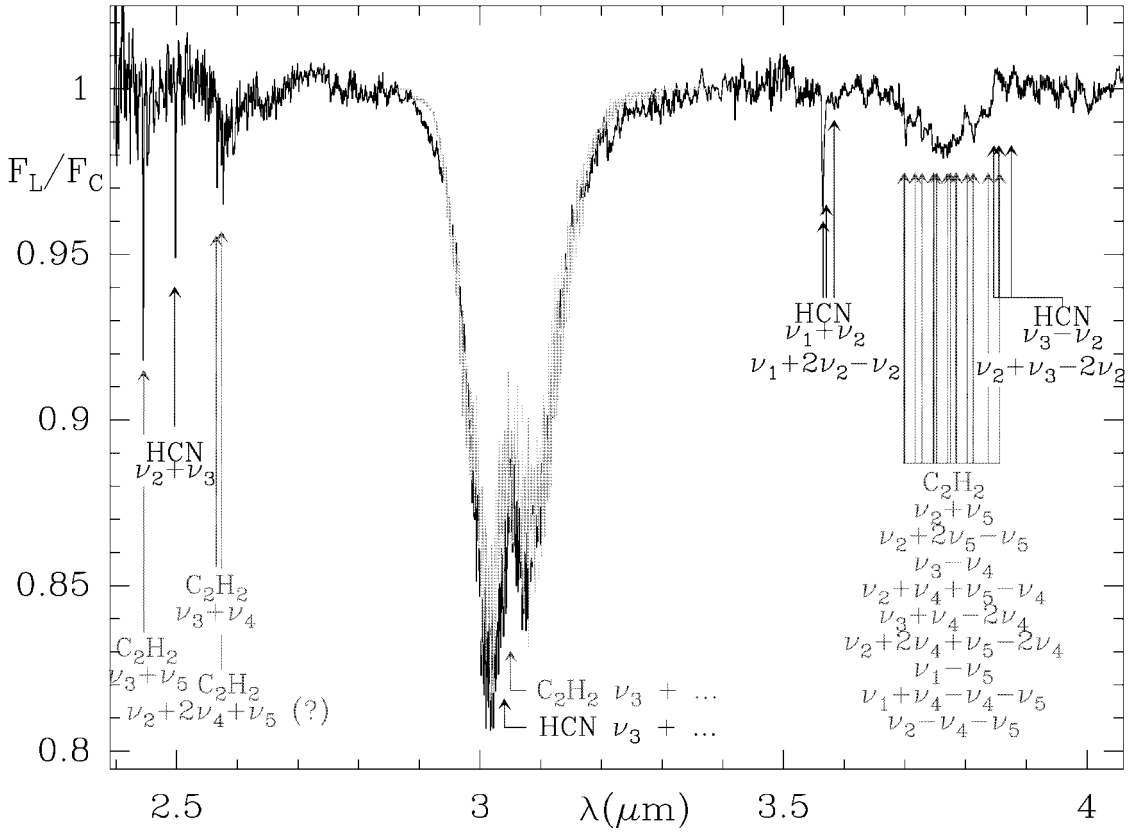

FIG. 2.—Observed spectrum between 2.4 and 4.0 μm in IRC +10216. The spectral resolution is $\simeq$150 km s^{-1}. The thin line shows the modeling of the C_2H_2 and HCN stretching mode at 3 μm and their hot and combination bands. The positions of the bands are indicated by arrows.

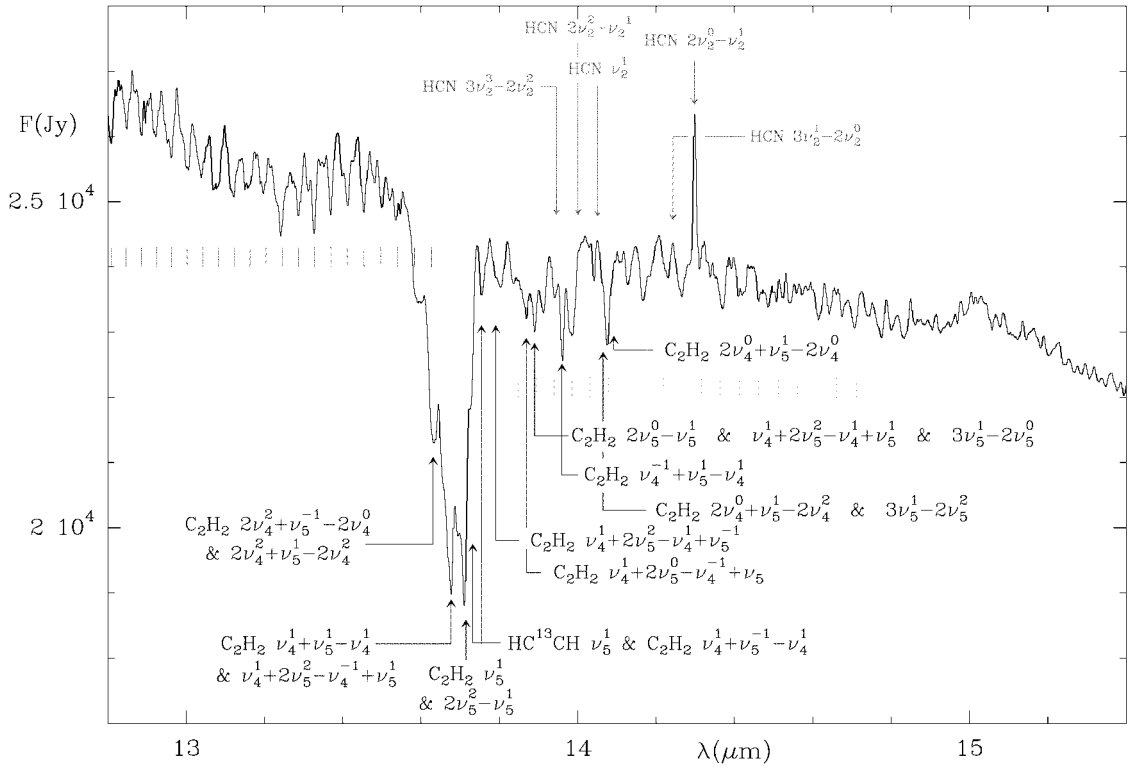

FIG. 3.—Observed spectrum around 15 μm. The spectral resolution is ~200 km s^{-1}. The position of the bands are indicated. Vertical lines indicate the positions of the individual *R* and *P* lines of the fundamental bending mode of C_2H_2. Note that the HCN bands are in emission as indicated by the shape of the *P*-branch of C_2H_2 relative to the *R* one and by the strong *Q*-branch of the $2\nu_2$ $l = 0$–ν_2 $l = 1$ transition.

order to fit the wings of the 3 μm feature, we have included an additional contribution from a warm gas in the inner region ($T_K \approx 1700$ K; $1 < r < 3R_*$). The C_2H_2 and HCN abundances in this layer are 2.5×10^{-5} and 1.5×10^{-5}, respectively. This layer could be similar to the warm molecular envelope found by Tsuji et al. (1997) and Yamamura et al. (1999) in other CSEs, and its origin is probably related to the pulsation of the central star (Woitke et al. 1999). Observations of high-*J* lines of C_2H_2 and HCN with much better spectral and angular resolution are needed to infer the structure of the inner envelope and the abundance of both molecular species. Fuente, Cernicharo, & Omont (1998) have derived an abundance ratio C_2H_2/HCN $\simeq$ 1 from observations of CCH and HCN. This value corresponds to the external layers of the CSE in which CCH is observed.

The HCN emission has to be modeled in a more complicated way. The ν_3 band of HCN at 3 μm, although contaminated by C_2H_2, seems to be in absorption, whereas the bending states are detected in emission against the continuum. The *Q*-branch of the $2\nu_2^0$–ν_1^1 band is particularly strong, in part due to low-velocity separation between the individual lines ($\simeq$0.4 km s^{-1}). All the other *Q*-branches (ν_2^1, $2\nu_2^2$–ν_2^1, $3\nu_2^1$–$2\nu_2^0$) also appear in emission, but are weaker. P Cygni profiles are in fact expected for HCN and C_2H_2 (Wiedemann et al. 1991). The larger beam size of the SWS compared to the high angular resolution data of Wiedemann et al. could favor the observation of reemission from HCN through resonant scattering in the molecular envelope. Obviously the same could happen for acetylene. The different behavior of both molecules must be related to the larger abundance of C_2H_2 through the whole envelope (which increases the importance of stellar blocking and absorption by the dust due to the larger number of absorption and remission processes; see González-Alfonso & Cernicharo 1999a, 1999b) and/or to the excitation mechanism that gives rise to the HCN band emission. An important difference between both molecules would be established if ro-vibrational excitation is mainly radiative instead of collisional: while the $2\nu_2^0$ state of HCN is radiatively connected to the ground state, the equivalent transition in C_2H_2 is forbidden, i.e., no photons can be absorbed from the ground to the $2\nu_5^0$ state due to the fact that both levels have the same symmetry (σ_g^+). In HCN, photons absorbed from the ground to the $2\nu_2^0$ level will decay preferentially to the ν_2^1 level, because this transition has an Einstein coefficient for spontaneous emission of ~4 s^{-1}, i.e., twice the value corresponding to the decay to the ground state. The equivalent process in C_2H_2 is radiative excitation from the ground to the $\nu_4+\nu_5$ state followed by radiative decay to the ν_4 level. However, this transition is very close in frequency to the *Q*-branch of the ν_5 transition, and any possible reemission could not compensate for the strong absorption from the ground to the ν_5 bending mode.

With the use of the nonlocal, non-LTE code described by González-Alfonso & Cernicharo (1997), we have modeled the HCN emission/absorption in IRC +10216. The rotational transitions of $2\nu_2+\nu_3$ ($l = 0$, 2), $\nu_2+\nu_3$, ν_3, $\nu_3+\nu_2$–ν_2, ν_3–ν_2, $2\nu_2$ ($l = 0$, 2), ν_2, $2\nu_2$–ν_2, and $3\nu_2$–$2\nu_2$ bands of HCN have been calculated using the rotational constants and transition dipole moments for these bands from Maki et al. (1996), Smith et al. (1989), Kim & King (1979), and Smith (1981). We have adopted a mass-loss rate of 1.5×10^{-5} $M_\odot$ yr^{-1} (Cernicharo et al. 1996).

The results (see Fig. 4) predict that the ν_3, $\nu_3+\nu_2$, and $2\nu_2$

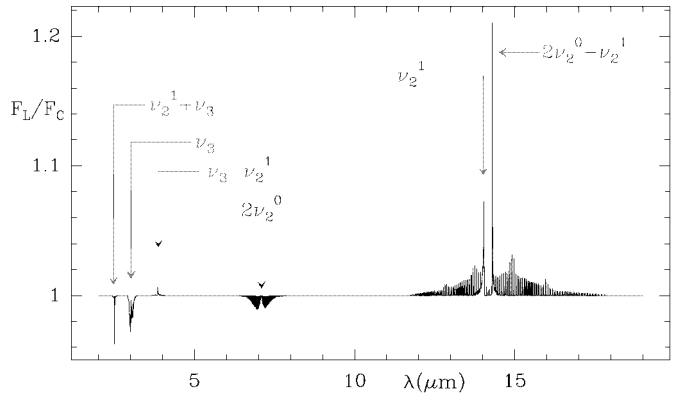

FIG. 4.—Modeled HCN spectrum in IRC +10216. The model is described in the text. Note the large intensity predicted for the *Q*-branch of the $2\nu_2$ $l = 0$–ν_2 $l = 1$ transition, in good agreement with the observations. In addition, the ν_3-ν_2^1) band is also predicted in emission as observed in Fig. 1.

bands of HCN will be in absorption while the ν_2 and its overtone bands will be in emission. The model also predicts that the ν_3–ν_2 band will be in emission. In fact, a detailed analysis of Figure 2 shows that this band appears indeed in emission. With the adopted HCN abundance (3×10^{-5} from Cernicharo et al. 1996), which matches the HCN rotational emission from a more simple large velocity gradient analysis, the *Q*-branch emission of the $2\nu_2^0$–ν_2^1 transition is overestimated by a factor of ≈2, so that a better estimate of the HCN abundance would be ∼(1–1.5) × 10^{-5}. The pumping mechanisms are different for the different regions of the envelope. In the innermost regions, before the dust formation zone, absorption of photons at 3 μm in the ν_3 mode will be very efficient. Radiative decay to the $2\nu_2$ $l = 0$ and ν_2 $l = 1$ states will be an important mechanism to populate both levels. Also in this region the ν_3–ν_2 band will appear in emission. Outside the dust formation region the flux at 3 μm decreases, but it increases considerably at 7.1 μm. The pumping from the ground state to the $2\nu_2$ $l = 0$ vibrational level, followed by radiative decay to the ν_2 $l = 1$ level, will be the main mechanism in producing the observed emission at 14.3 μm. Consequently, the intensity of the HCN bands, as observed by *ISO*, will be very different in stars with low, moderate, or high mass-loss rates (see, e.g., Aoki, Tsuji, & Ohnaka 1999). Our calculations show that resonant scattering through the envelope is very efficient for HCN and also probably for C_2H_2 (see Cernicharo 1998; González-Alfonso et al. 1998 have modeled similar effects for water vapor). Resonant scattering in CSEs could also have an effect on the heating and cooling of the molecular gas (Cernicharo 1998). The behavior of the observed HCN emission bands is similar to that found in O-rich stars by Justtanont et al. (1998) for CO_2; in fact, González-Alfonso & Cernicharo (1999a, 1999b) have shown that the CO_2 emission around 15 μm could also be explained by resonant scattering through the CSEs. The radiative pumping mechanism for HCN was already mentioned by Lucas & Cernicharo (1989) to explain the strong $\nu_2 = 1$ $J = 2$–1 maser in IRC +10216 and other C-rich CSEs. Our calculations indicate that the low-*J* lines of the $\nu_2 = 1$ vibrational state are inverted and that the proposed radiative pumping could explain the maser emission. However, the ro-vibrational lines of the *Q*-branch are overlapped in frequency, and these effects have to be considered in order to explain the millimeter and submillimeter masers of HCN (see, e.g., González-Alfonso & Cernicharo 1997).

J. C. and E. G.-A. acknowledge Spanish DGES for this research under grants PB96-0883 and ESP98-1351E.

REFERENCES

Aoki, W., Tsuji, T., & Ohnaka, K. 1999, A&A, 345, 945
Boyle, R. J., Keady, J. J., Jennings, D. E., Hirsch, K. L., & Wiedemann, G. R. 1994, ApJ, 420, 863
Cernicharo, J. 1998, Ap&SS, 255, 303
Cernicharo, J., et al. 1996, A&A, 315, L201
Cernicharo, J., Gottlieb, C. A., Guélin, M., Thaddeus, P., & Vrtilek, J. M. 1989, ApJ, 341, L25
Cernicharo, J., & Guélin, M. 1987, A&A, 183, L10
———. 1996, A&A, 309, L27
Cernicharo, J., Guélin, M., Bogey, M., Demuynck, C., & Destombes, J. L. 1991, A&A, 246, 213
Cernicharo, J., Guélin, M., & Kahane, C. 1999, A&A, in press
de Graauw, T., et al. 1996, A&A, 315, L49
Fuente, A., Cernicharo, J., & Omont, A. 1998, A&A, 330, 232
González-Alfonso, E., & Cernicharo, J. 1997, A&A, 322, 938
———. 1999a, in The Universe as Seen by *ISO*, ed. P. Cox & M. Kessler (ESA SP-427; Noordwijk: ESA), 325
———. 1999b, ApJ, 525, 845
González-Alfonso, E., Cernicharo, J., van Dishoeck, E. F., Wright, C. M., & Heras, A. 1998, ApJ, 502, L169
Guélin, M., Lucas, R., & Cernicharo, J. 1993, A&A, 280, L19
Justtanont, K., Feuchtgruber, J., de Jong, T., Cami, J., Waters, L. B. F. M., Yamamura, I., & Onaka, T. 1998, A&A, 330, L17
Keady, J. J., & Hinkle, K. H. 1988, ApJ, 331, 539
Keady, J. J., & Ridway, S. T. 1993, ApJ, 406, 199
Kim, K., & King, W. T. 1979, J. Chem. Phys., 71, 1967
Lucas, R., & Cernicharo, J. 1989, A&A, 218, L20
Maki, A., Quapp, W., Klee, S., Mellau, G. C., & Albert, S. 1996, J. Mol. Spectrosc., 180, 323
Ridgway, S. T., Carbon, D. F., & Hall, D. N. B. 1978, ApJ, 225, 138
Rinsland, C. P., Baldacci, A., & Rao, K. N. 1982, ApJS, 49, 487
Smith, I. W. M. 1981, J. Chem. Soc. Faraday Trans., 77, 2357
Smith, M. A. H., Coy, S. L., Klemperer, W., & Lehmann, K. K. 1989, J. Mol. Spectrosc., 134, 134
Tsuji, T., Ohnaka, K., Aoki, W., & Yamamura, I. 1997, A&A, 320, L1
Wiedemann, G. R., Hinkle, K. H., Keady, J. J., Deming, D., & Jennings, D. E. 1991, ApJ, 382, 321
Woitke, P., Helling, Ch., Winters, J. M., & Jeong, K. S. 1999, A&A, 348, L17
Yamamura, I., de Jong, T., Justtanont, K., Cami, J., & Waters, L. B. F. M. 1998, Ap&SS, 255, 351
Yamamura, I., de Jong, T., Waters, L. B. F. M., Cami, J., & Justtanont, K. 1999, in IAU Symp. 191, Asymptotic Giant Branch Stars, ed. T. Le Bertre, A. Lébre, & C. Waelkens (San Francisco: ASP), 267